

COMPLEX PERMEABILITY SPECTRA OF MANGANESE-ZINC FERRITE AND ITS COMPOSITE

Rastislav Dosoudil — Vladimír Olah *

The magnetic permeability spectra of an Mn-Zn sintered ferrite and its composite have been studied. The model based on the relaxation-type spin resonance formulation combined with the magnetic circuit model for ferrite magnetocomposites was proposed. The relevance of this model has been verified by measuring of the complex permeability of the composite and compared to the properties of the sintered ferrite. The observed relaxation frequencies of the composite are much higher than those of the sintered material.

Key words: complex permeability, composite magnetic material, magnetic circuit, spin resonance, sintered ferrites

1 INTRODUCTION

The sintered ferrites have frequency-dependent permeabilities. For polycrystalline ferrites, the permeability is related to the following magnetizing mechanisms: the spin rotation and domain wall motion. There have been many studies of the permeability of polycrystalline ferrites [2, 5-7].

The magnetic composite materials (magnetocomposites) can be denoting as materials of the future because of their advantageous properties [9]. Magnetocomposites consist of two basic parts: ferrite magnetic particles (magnetic filler) with appropriate morphology (shape) and granulometry (sizes D , d and volume fraction ν_i) that are responsible for magnetic properties of composites and polymer matrix, the properties of which determine the homogeneity of magnetic particles arrangement in the composite, and non-magnetic properties of composite materials (mechanical, chemical, rheological, etc). The permeability values and their frequency dependence can be con-

trolled by the fabrication process of the magnetocomposites. In the case of magnetocomposites, we consider the magnetic permeability as an effective parameter [8, 9, 10].

2 PROBLEM FORMULATION AND MODEL DESCRIPTION

The effective permeability in ferrite magnetocomposites can be generally estimated using for example the effective medium theory [4, 7], the percolation theory [3] and/or magnetic circuit model [2, 5, 8, 9, 10], etc. In this study, the magnetic circuit model approach has been used. The main advantage of this approach is simplicity and good agreement with an experiment.

2.1 Magnetic circuit model

We consider the ferrite magnetocomposites to be composed of prismatic magnetic particles (with intrinsic permeability μ_i) surrounded by a non-magnetic polymer

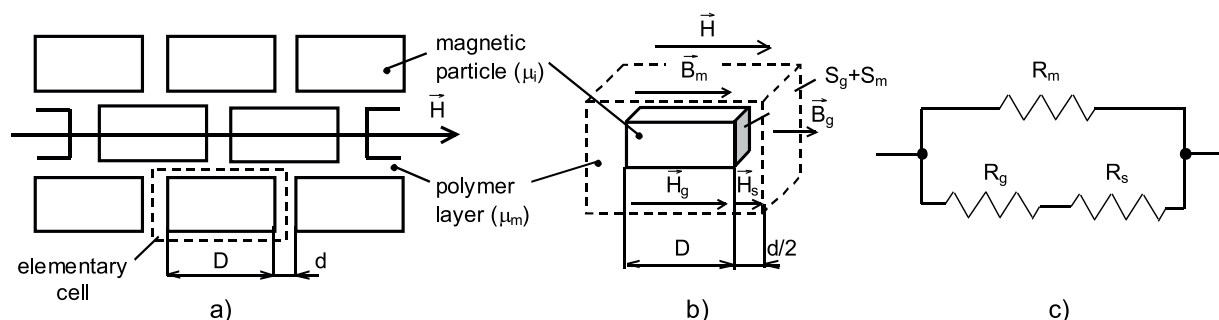


Fig. 1. Schematic representation of magnetocomposite: a) magnetic particles arrangement in polymer matrix, b) elementary cell, and c) equivalent magnetic circuit of elementary cell

* Department of Electromagnetic theory, Ilkovičova 3, 812 19 Bratislava, Slovakia, E-mail: dosoudil@elf.stuba.sk

layer ($\mu_m \ll \mu_i$). The schematic configuration is shown in Fig. 1a,b. The elementary cell of idealized composite structure is modelled using series-parallel magnetic circuit (Fig. 1c), [8, 10].

In this magnetic circuit is particle reluctance R_g in series connection together with polymer gap reluctance R_s and both ones bridged by parallel reluctance R_m of matrix layer around the particle. The average size of the magnetic particles and the average thickness of the non-magnetic polymer layer are denoted by D and d , respectively. There are two magnetic resistivities: intraparticle resistivity (grain boundary) and interparticle resistivity (polymer layer). The magnetic resistivity of the polymer layer is much higher than that of the grain boundary in the magnetic particle. We assume the following conditions: $d \ll D$, magnetic fluxes Φ_g and Φ_m passing through both parallel circuit branches are homogeneous, and relative high particle (volume) concentration. Then the Ampère's integral (we neglect the resistivity of the grain boundary in the magnetic particles) applied to the branch with series connected reluctances (R_g and R_s) states:

$$\int_0^{D+d} \vec{H} d\vec{l} = \int_0^D \vec{H}_g d\vec{l} + \int_0^{D+d} \vec{H}_s d\vec{l} \\ \implies H_g D + H_s d = H(D+d) (\equiv NI) \quad (1)$$

where H is the external applied field intensity, H_g and H_s are the magnetic field intensities of particle and polymer, respectively, and \vec{H} , \vec{H}_g and \vec{H}_m are the corresponding vectors. We assume that H_g and H_s are constant in particle and matrix, respectively. N is a number of coil turns surrounding a toroidal sample and I is an effective value of ac current flowing through the coil. For the elementary magnetic circuit the effective magnetic flux density B_e can be calculated from the next equation:

$$\iint_{S_g+S_m} \vec{B}_e d\vec{S} = \iint_{S_g} \vec{B}_g d\vec{S} + \iint_{S_m} \vec{B}_m d\vec{S} \\ \implies B_e = \left(\frac{NI}{R_g + R_s} + \frac{NI}{R_m} \right) \frac{1}{S} \quad (2)$$

where B_g and B_m are the magnetic flux densities in the magnetic particle and polymer, respectively, \vec{B}_g and \vec{B}_m are the corresponding vectors, and the area S is given by the summation of the cross-sections of magnetic particle S_g and polymer matrix S_m : $S = S_g + S_m$. Using the Eq. (1) and Fig. 1 we can write the equation (2) in the following form ($\mu_m \approx 1$):

$$B_e = \mu_o \mu_e H = \mu_o \left\langle \frac{\mu_i \left(1 + \frac{d}{D}\right)}{\left(1 + \mu_i \frac{d}{D}\right) \left(1 + \frac{S_m}{S_g}\right)} + \frac{1}{1 + \frac{S_g}{S_m}} \right\rangle \quad (3)$$

from which results:

$$\mu_e = \left\langle 1 + \frac{\chi_i(1+\eta)}{1+\mu_i\eta} \nu_i \right\rangle \quad (4)$$

where $\langle \rangle$ means a statistical mean value and $\mu_i(\chi_i)$ is the intrinsic permeability (susceptibility) of magnetic particles, $\eta = d/D$ is so-called 'demagnetising structural parameter' and $\sigma = S_m/S_g$ is so-called 'area (cross-sectional) structural parameter'. Both structural parameters have statistical characters (distributions) and are connected through the volume particle fraction: $\nu_i = 1/[(1+\eta)(1+\sigma)]$. Equation (4) expresses an influence of granulometry (sizes D and d) and composite density (volume fraction ν_i) on the effective permeability value μ_e . In this approach we also assumed that D and d do not change with the frequency of an external magnetic field and that the intrinsic permeability of the magnetic particle is almost equal to that of the sintered ferrite (μ_i).

2.1 Frequency dispersion of the effective permeability

When a magnetic material is subjected to a change in the applied magnetic field there are time-dependent effects to consider as the magnetic moments reorient and the domain walls move. Then two types of (ferromagnetic) resonance may occur. These are a spin resonance based on the Landau-Lipschitz-Gilbert (electromagnetic torque) equation for spin dynamics [1]:

$$\frac{\partial \vec{M}}{\partial t} = -\gamma \mu_o \vec{M} \times \vec{H} + \frac{4\pi\lambda_d}{\gamma \mu_o M^2} \left(\vec{M} \times \frac{\partial \vec{M}}{\partial t} \right) \quad (5)$$

and a domain-wall resonance based on the equation of motion of the domain walls, the damped simple harmonic oscillator equation describing motion of a planar 180°-domain wall in magnetic material (*ie* also in magnetic particles):

$$m_w \frac{d^2 x(t)}{dt^2} + \beta \frac{dx(t)}{dt} + k_w x(t) = 2\mu_o \vec{M}_s \cdot \vec{H} \quad (6)$$

where \vec{M} is the magnetization vector, \vec{H} is the magnetic field intensity vector, λ_d is the relaxation frequency, γ is the gyromagnetic ratio, $x(t)$ is the position of domain wall, m_w is the effective mass of domain wall per unit of area (m_w relates the acceleration of the domain wall to the force causing acceleration), β is the damping coefficient which is determined by the combined effect of all energy dissipation mechanisms, k_w is the stiffness (or restoring force) coefficient, \vec{M}_s is the saturation magnetization vector and t is the time.

Equation (5) is more widely used in the description of spin dynamics, and in fact it is a generalization of the Landau-Lipschitz equation, since the latter can be derived from this equation by neglecting the higher-order terms in the expression for $\partial \vec{M} / \partial t$ on the right-hand side of

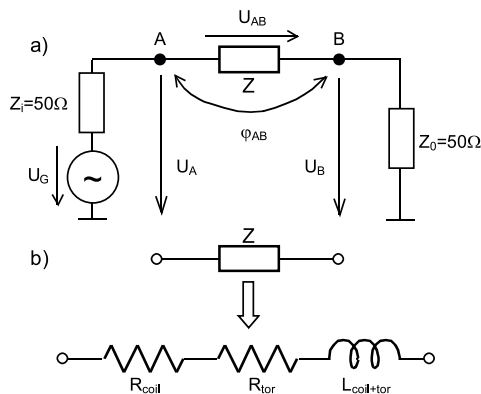


Fig. 2. HF measurement: a) measuring circuit (1 MHz to 1 GHz) and b) series model of measured impedance

the equation. Critical damping of the motion of the magnetic moments occurs when $\lambda_d = \gamma\mu_o M/4\pi$. For values of $\lambda_d \ll \gamma\mu_o M/4\pi$ the spins perform a number of precessions before finally reaching the field direction, while for $\lambda_d \gg \gamma\mu_o M/4\pi$ the spins will rotate slowly but directly toward the field direction. The value of this relaxation frequency λ_d for materials such as nickel-zinc ferrite and manganese-zinc ferrite is typically $10^7 - 10^8 \text{ s}^{-1}$. This relaxation frequency is insufficient to reach critical damping.

At low driving fields the Eq. (6) assumes that the moving domain wall remains flat during its motion (we neglect ‘bowing’ and ‘pinning’ effects). Under certain conditions, when the motion of the domain walls is lightly damped so that $\beta^2 < 4m_w k_w$, the motion of the domain walls can exhibit resonance. When damping is heavy, so that $\beta^2 > 4m_w k_w$, the domain walls will simply exhibit relaxation. Critical damping occurs when $\beta_2 = 4m_w k_w$ leading to the fastest approach to equilibrium.

For polycrystalline ferrites, the effective permeability spectrum can be described by the superposition of two components that can be attributed to two types of magnetizing processes, spin rotation and domain wall motion [1, 2, 6]:

$$\tilde{\mu}_e(\omega) = 1 + \tilde{\chi}_{e,\text{spin}}(\omega) + \tilde{\chi}_{e,\text{wall}}(\omega). \quad (7)$$

We assume that the spin rotation component $\tilde{\chi}_{e,\text{spin}}$ is relaxation type:

$$\tilde{\chi}_{e,\text{spin}}(\omega) = \frac{\chi_{i,\text{spin}}}{1 + j\frac{\omega}{\omega_{\text{res}}}} \quad (8)$$

and that the domain wall component $\tilde{\chi}_{e,\text{wall}}$ is resonance type:

$$\tilde{\chi}_{e,\text{wall}}(\omega) = \frac{\chi_{i,\text{wall}}\omega_{\text{wall}}^2}{\omega_{\text{wall}}^2 - \omega^2 + j\frac{\beta}{m_w}\omega} \quad (9)$$

where $\chi_{i,\text{spin}}$ and ω_{res} correspond to the static spin susceptibility and the spin resonance frequency, respectively,

$\chi_{i,\text{wall}}$ and ω_{wall} are the static susceptibility of the domain wall motion and the domain wall resonance frequency. Equation (8) was derived from Eq. (5) and represents the well-known Debye relaxation formula. Resonance formula — Eq.(9) was derived from Eq.(6) with respect to each of term.

In the case of magnetocomposites, it can be used only the relaxation-type of spin resonance formulation — Eq. (8). For constant magnitude of the harmonic applied field, the combination of Eqs. (8) and (4) gives the relation of the complex effective permeability as

$$\tilde{\mu}_e(\omega) = \left\langle 1 + \frac{\chi_{i,\text{spin}}(1 + \eta)\nu_i}{(1 + \mu_{i,\text{spin}}\eta)\left(1 + j\frac{\omega}{\omega_{\text{res}}(1 + \mu_{i,\text{spin}}\eta)}\right)} \right\rangle \quad (10)$$

where $\mu_{i,\text{spin}}$ is the static spin permeability of magnetic particles in the magnetocomposites. As we will show in the next section, it cannot be used the Eq. (9) attributed to the domain wall motion in the whole frequency range (10 kHz to 1 GHz for measured magnetocomposite sample). The frequency dispersion of complex effective permeability in magnetocomposites can be described using only the spin resonance formulation.

3 EXPERIMENTAL

3.1 Sample preparation

We had prepared Mn-Zn sintered ferrite samples in a toroidal form (dimensions: outer diameter 10, inner diameter 6 and height 4 mm, type H21 — produced by S+M Components Šumperk, Czech Republic) with Curie temperature $T_c > 476 \text{ K}$, mass density 4.8 gcm^{-3} , intrinsic permeability $\mu_i = 1900 \pm 20 \%$. The used manganese-zinc sintered ferrite consists of 37 wt.% MnO, 12 wt.% ZnO and 51 wt.% Fe₂O₃ (composition: $\approx \text{Mn}_{0.37}\text{Zn}_{0.57}\text{Fe}_{2.06}\text{O}_4$). Magnetic particles, prepared by mechanical granulation of Mn-Zn ferrite (H21), with two fractions: (25–40) + (250–315) μm at the ratio of fractions 1 : 1.5, were used for preparation of magnetocomposites with non-magnetic matrix. In our case, the polymer matrix was thermoelastoplastic blend TPE (Finaprene 416, Krasten 126, Miravithen D14003 and oil OLM4). The ferrite filler and polymer matrix were thermally processed at a temperature of 436 K and then thermally pressed at a pressure of 17 MPa into a plate form from which were cut out the toroidal samples with dimensions $10 \times 5 \times 5.5 \text{ mm}$. The mass concentration of ferrite filler in the composites was $\kappa = 93 \text{ wt.}\%$ (*ie* volume concentration $\kappa_v = 72.2 \%$).

3.2 Measuring methods

The complex effective permeability ($\tilde{\mu}_e = \mu_{e1} - j\mu_{e2}$) of the samples were measured by two different techniques. In the frequency range 1 kHz to 5 MHz, $\tilde{\mu}_e$ was obtained by measuring the inductance (ωL) and the resistance (R)

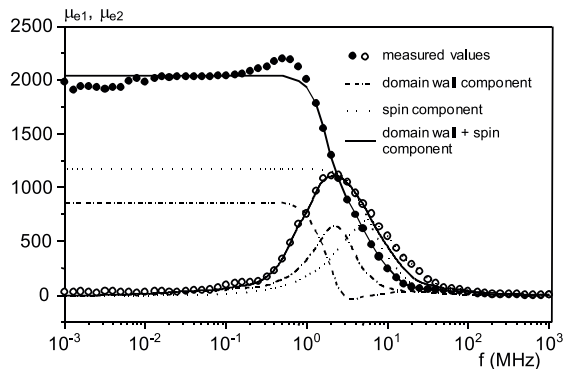


Fig. 3. The frequency dependencies of real and imaginary parts of complex effective permeability for sintered Mn-Zn ferrite

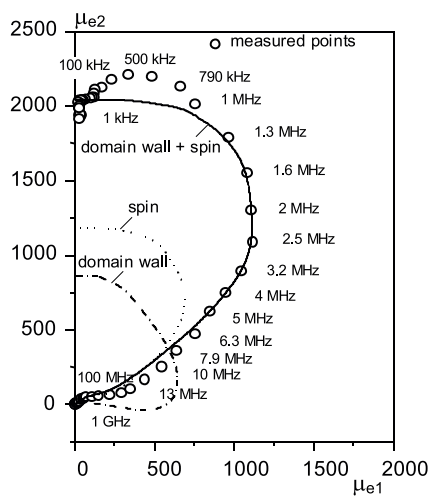


Fig. 4. The frequency spectrum of complex effective permeability for sintered Mn-Zn ferrite

differences between a toroidal coil wound (with number of turns $N = 1$) around the toroidal (sintered ferrite or magnetocomposite) sample and one wound without the toroidal sample, using the low-frequency impedance tester HIOKI 3531 Z HiTester with constant effective value of driving voltage ≈ 50 mV (in series mode). In the frequency range 1 MHz to 1 GHz, $\tilde{\mu}_e$ was obtained by measuring the input and output rms voltages U_A and U_B together with phase angle (shift) φ_{AB} between both voltages by the vector voltmeter Hewlett Packard 4205A (coaxial line technique, Fig. 2). The experimental error for the complex effective permeability in the frequency range 1 kHz to 100 MHz is less than 6% and over 100 MHz less than 12%.

For a series model of the measured impedance \mathcal{Z} , the following equations can be derived:

$$R_{\text{coil}} + R_{\text{tor}} + j\omega L_{\text{coil+tor}} = j\omega \mu_o S_{\text{tor}} (\mu_{e1} - j\mu_{e2}) \frac{N^2}{l_s} \quad (11)$$

$$\mu_{e1} = \frac{l_s(L_{\text{coil+tor}} - L_{\text{coil}})}{\mu_o S_{\text{tor}} N^2} \quad (12)$$

$$\mu_{e2} = \frac{l_s(R_{\text{coil+tor}} - R_{\text{coil}})}{\mu_o \omega S_{\text{tor}} N^2} \quad (13)$$

where R_{coil} and ωL_{coil} are the series resistance and inductance of a toroidal coil wound without the toroidal sample, R_{tor} and ωL_{tor} are the series resistance and inductance that represent magnetic losses in the toroidal sample, $R_{\text{coil+tor}} = R_{\text{coil}} + R_{\text{tor}}$, $L_{\text{coil+tor}} = L_{\text{coil}} + L_{\text{tor}}$, and S_{tor} and l_s are the cross-section and the mean length of the toroidal sample, respectively. Since for $\omega \rightarrow 0$ is $\mu_{e2}(\omega) \rightarrow \infty$, we had to use for verification of $\mu_{e2}(\omega)$ values in low-frequency region (below 100 kHz) Kramers-Kronig relation, [1], [11]:

$$\mu_{e2}(\omega) = \frac{2}{\pi} \int_0^{\infty} \mu_{e1}(s) \frac{\omega}{\omega^2 - s^2} ds. \quad (14)$$

4 RESULTS AND DISCUSSION

The frequency dependencies of the real and imaginary parts of complex effective permeability for the sintered ferrite are shown in Fig. 3. For sintered Mn-Zn ferrite, the real part μ_{e1} , which is about 2000 in the low-frequency region, begins to decrease at about 1 MHz, and reaches the value of about 12 at 100 MHz. On the other hand, the imaginary part μ_{e2} has a maximum of about 1100 at around 2.5 MHz. From the numerical fitting of the frequency dependencies of μ_{e1} and μ_{e2} for the sintered ferrite to the equations (7)–(9), we obtained the set of the parameters as $\chi_{i,\text{spin}} = 1199$ and $\omega_{\text{res}} = 4.02 \times 10^7 \text{ s}^{-1}$ (6.4 MHz) for the spin rotation component, and the set $\chi_{i,\text{wall}} = 861$, $\omega_{\text{wall}} = 1.59 \times 10^7 \text{ s}^{-1}$ (2.53 MHz) and $\beta/m_w = 2.35 \times 10^7 \text{ s}^{-1}$ (3.74 MHz) for the domain wall motion. Using Eqs. (7)–(9) with these parameters, we calculated the complex effective permeability spectrum (in the complex plane) for the sintered manganese-zinc ferrite, which is shown in Fig. 4. Each calculated spectrum of spin rotation and domain wall motion is also shown in this figure. Good agreement between experimental data and calculation curves was obtained only above the frequency of 1.3 MHz. The complex effective permeability in high-frequency region above 6 MHz can be describing with the spin rotation component.

The frequency dependencies of μ_{e1} and μ_{e2} for the magnetocomposite sample are shown in Fig. 5. For this sample, the real part μ_{e1} , which is about 14 in the low-frequency region, begins to decrease at about 100 MHz. The imaginary part μ_{e2} has a maximum of about 7.8 at around 400 MHz.

From the numerical fitting of the dependencies of $\mu_{e1}(\omega)$ and $\mu_{e2}(\omega)$ to the equation (10), we obtained the next set of the fitting (dispersion) parameters: $\chi_{i,\text{spin}} = 1199$ and $\omega_{\text{res}} = 2.69 \times 10^9 \text{ s}^{-1}$ (429 MHz) for the spin rotation component. Using Eq. (10) with these parameters, we calculated the complex frequency spectrum of the

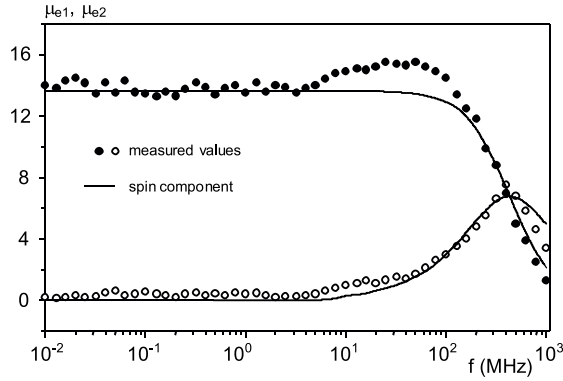


Fig. 5. The frequency dependencies of real and imaginary parts of complex effective permeability for magnetocomposite

effective permeability (Fig. 6) for spin rotation. We can state that it was obtained good consensus between experimental results and those obtained from our proposed model.

In this case, it cannot be used in the frequency range 10 kHz to 1 GHz the Eq. (9) attributed to the domain wall motion. However, the effective permeability spectrum in this frequency region cannot be realized by considering the contributions of both the domain wall motion and the spin rotation. Thus the effective permeability in this frequency region can be reproduced only with the spin rotation component. This discrepancy can be regarded as the microstructure difference between the sintered Mn-Zn ferrite and the magnetic ferrite particles in magnetocomposites. Since the dispersion parameters of domain wall motion ($\chi_{i,wall}$, ω_{wall} , β/m_w) are sensitive to the microstructure of the polycrystalline ferrite, the parameters obtained in the sintered ferrite cannot be applied to calculate the parameters of magnetocomposites. Therefore, it is necessary to evaluate the microstructure both of the sintered ferrite and ferrite particles in the magnetocomposites in order to consider the contribution of the domain wall motion.

In ferrite magnetocomposites, a magnetic inert component is introduced that causes not only the magnetic dilution but also a cut-off the magnetic circuit in the ferrite. Therefore, the permeability is reduced remarkably as the ferrite volume loading decreases. We consider three configurations of magnetic connection changes: (a) the sintered ferrite sample (volume fraction 1), (b) the magnetocomposite sample with high volume loading and (c) with low volume loading (Fig. 7). The magnetic gaps in the sintered ferrite sample can be negligible, so that the magnetic moment is easily aligned along an applied field. In the magnetocomposite sample with high volume loading, some magnetic particles aggregate to form a magnetic cluster and the magnetic poles on the surface of the cluster create the demagnetising field antiparallel to the applied field.

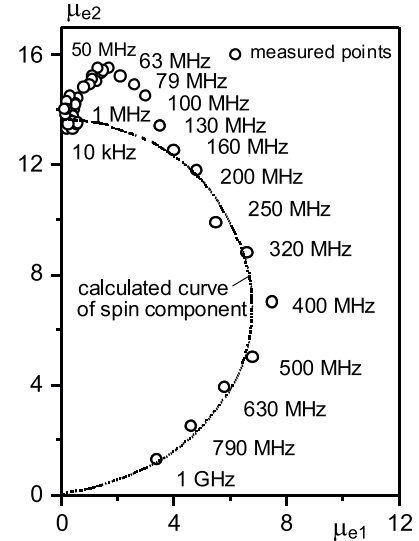


Fig. 6. The frequency spectrum of complex effective permeability for magnetocomposite

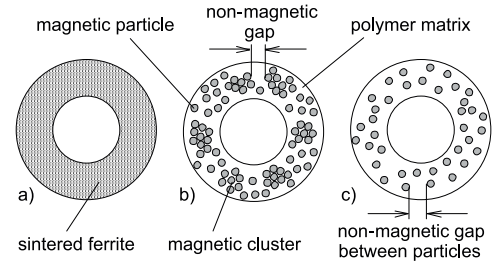


Fig. 7. Schematic configurations of: (a) sintered ferrite toroidal sample, (b) magnetocomposite toroidal sample with high ferrite content and (c) with low ferrite content

Further, low volume loading composite sample have magnetic particles separated individually, and the magnetic poles on each particle generate the demagnetising field. The demagnetising field reduces the induced magnetic moment more than that calculated from the volume loading. Therefore, the permeability in low-frequency region decreases with the configuration change from the sintered ferrite to the magnetocomposites. On the other hand, the spin resonance frequency ω_{res} is represented by the equation [1,6]: $\omega_{res} = \gamma\mu_o H_a$, where H_a is the effective anisotropy field which is written by the summation of the magnetocrystalline anisotropy field and the shape anisotropy field. The former is determined by the composition and the crystal structure of the magnetic component, and the latter depends on the particle shape and the particle configuration. For the sintered ferrite, the contribution of the magnetocrystalline field is larger than that of the shape anisotropy field, since the magnetic gaps can be negligible.

For the magnetocomposites consisting of isotropic (polyhedral) shape particles, there are some aggregates in the case of high volume loading and the particles are

dispersed individually in the case of low volume loading. Since the cluster of the magnetic particles responds as a magnetic unit, the number of magnetic poles per unit volume is less than that for isolated particles. Therefore, the shape anisotropy field is introduced, which is equivalent to the demagnetising field H_d induced by the rf magnetic field. The spin resonance frequency can then be modified by: $\omega_{\text{res}} = \gamma\mu_o(H_a + H_d)$. In the case of magnetocomposites, the demagnetising field increases with decreasing volume loading. The spin resonance frequency shifts higher due to the contribution of the demagnetising field. As the result, the $\mu_{e1}(\omega)$ can take a larger value than that of the sintered ferrite in the rf frequency region.

5 CONCLUSION

We have studied the frequency spectra of the complex effective permeability for manganese-zinc sintered ferrite and its magnetocomposite using the spin and domain wall resonance formulation combined with the magnetic circuit model. The model analysis includes the effect of the demagnetising field and the volume loading of the ferrite in the magnetocomposite. In the Mn-Zn ferrite magnetocomposite, the real part of the complex effective permeability in the high-frequency region (above 100 MHz) becomes larger than that of the sintered ferrite. This is attributed to the shift of the spin resonance frequency toward the higher frequency region by introducing a demagnetising field in the magnetocomposite. The model calculation is insufficient to evaluate the frequency spectra of the low-frequency complex effective permeability below about 5 MHz, even though the contribution of the domain wall motion is taken into account. This may be attributed to the difference between the domain structures of the sintered ferrite and the magnetic particles in the magnetocomposite. Since the dispersion parameters of the domain wall motion are sensitive to the microstructure of the polycrystalline ferrite, the parameters obtained in the sintered ferrite cannot be applied to calculate the parameters of composite material. Therefore, it is necessary to evaluate the microstructure both of the sintered ferrite particles and ferrite particles in the composite material in order to consider the contribution of the domain wall motion. Accordingly, further investigations are needed to understand the contribution of the domain wall motion. More detailed studies of the permeability dispersion in the low-frequency region are being carried out.

This work was supported by No. 1/7610/20 grant of VEGA agency of the Slovak Republic.

REFERENCES

- [1] SITIZE, Ju.—SATO, Ch.: Ferrites, Mir, Moscow, 1964. (in Russian)
- [2] NAKAMURA, T.—TSUTAOKA, T.—HATAKEYAMA, K.: Frequency Dispersion of Permeability in Ferrite Composite Materials, *J. of Magn. Magn. Mat.* **138** (1994), 319–328.
- [3] LAGARKOV, A. N.—SARYCHEV, A. K.—SMYCHKOVICH, Y. R.—VINOGRADOV, A. P.: Effective Medium Theory for Microwave Dielectric Constant and Magnetic Permeability of Conducting Stick Composites, *J. of Electromagnetic Waves and Applications* **6** No. 9 (1992), 1159–1176.
- [4] PATERSON, J. H.—DEVINE, R.—PHELPS, A. D. R.: *J. of Magn. Magn. Mat.* **196-197** (1999), 394–396.
- [5] JOHNSON, M. T.—VISSER, E. G.: A Coherent Model for the Complex Permeability in Polycrystalline Ferrites, *IEEE Trans. on Magn.* **26** No. 5 (1990), 1987–1989.
- [6] PARDAVI-HORVATH, M.: Microwave Applications of Soft Ferrites, *SMM 14/3/2 colb*, Sept. 13 (1999), 1–15.
- [7] GRIMES, C. A.—GRIMES, D. M.: Permeability and Permittivity Spectra of Granular Materials, *Phys. Rev. B* **43** No. 13 (1991), 10780–10788.
- [8] DOSOUDIL, R.: Modelling and Optimisation of Magnetic Properties of Polymer Magnetic Materials, PhD Thesis, Dept. of Electromagnetic Theory, STU, Bratislava, 2000.
- [9] SLÁMA, J.—GRUSKOVÁ, A.—KOVÁČIKOVÁ, S.—VICEN, R.—KRIVOŠÍK, P.—HUDEC, I.: Soft Magnetic Composite Properties Optimisation, *SMM 14*, Balatonfred, Hungary, Sept. 8-10 (1999), P2/3-327, 246.
- [10] SLÁMA, J.—GRUSKOVÁ, A.—KESZEGH, L.—KOLLÁR, M.: Magnetic Powder Filled Polymers, *IEEE Trans. Mag.* **30** (1994), 21101–1103.
- [11] FRANEK, J.: Causal Relation of the Frequency Spectra of the Hermitian and Anti-Hermitian Dispersion Matrix, *Proc. on the Conf.: "New Trends in Signal Processing"*, Liptovský Mikuláš, May 24-26 (2000), 350–354. (in Slovak)

Received 7 July 2000

Rastislav Dosoudil (Ing, PhD) was born in Bratislava, in 1970. He graduated from Faculty of Electrical Engineering, Slovak University of Technology, in Bratislava, in Material Engineering branch (Technology of Electronic Equipments), 1993 and received the PhD degree in Theory of Electromagnetism, in 2000. At present he is an Assistant Professor at the Department of Electromagnetic Theory. His research activity are mainly magnetocomposites materials and complex permeability phenomena.

Vladimír Olah (Ing) born in 1946, in Bratislava, Slovakia, graduated at Slovak University of Technology, Faculty of Electrical Engineering, in Bratislava, Czechoslovakia, in 1968. Since that time he has been working in an industrial plant TESLA Electroacoustics, at Institute for Technical Cybernetics of Slovak Academy of Science and in CHIRANA Star Tur as a development worker. Since 1990 till now he is with the Faculty of Electrical Engineering and Information Technology, Slovak University of Technology as a research worker. His activities concern the reliability of electrical materials, structures, components and circuits namely the properties of new magnetic materials.